



ARTICLE

Toward improved predictions of pharmacokinetics of transported drugs in hepatic impairment: Insights from the extended clearance model

Flavia Storelli¹ | Mayur K. Ladumor¹ | Xiaomin Liang² | Yurong Lai²  |
Paresh P. Chothe³ | Osatohanmwon J. Enogieru⁴ | Raymond Evers⁵ |
Jashvant D. Unadkat¹ 

¹Department of Pharmaceutics,
University of Washington, Seattle,
Washington, USA

²Drug Metabolism, Gilead Sciences
Inc., Foster City, California, USA

³Global Drug Metabolism and
Pharmacokinetics, Takeda
Development Center Americas, Inc.,
Lexington, Massachusetts, USA

⁴Pharmacokinetics & Drug Metabolism,
Amgen, South San Francisco,
California, USA

⁵Preclinical Sciences and Translational
Safety, Janssen Research &
Development, LLC, Spring House,
Pennsylvania, USA

Correspondence

Jashvant D. Unadkat, Department of
Pharmaceutics, School of Pharmacy,
University of Washington, 1959 NE
Pacific St, H272, Seattle, WA 98107,
USA.

Email: jash@uw.edu

Abstract

Hepatic impairment (HI) moderately (<5-fold) affects the systemic exposure (i.e., area under the plasma concentration–time curve [AUC]) of drugs that are substrates of the hepatic sinusoidal organic anion transporting polypeptide (OATP) transporters and are excreted unchanged in the bile and/or urine. However, the effect of HI on their AUC is much greater (>10-fold) for drugs that are also substrates of cytochrome P450 (CYP) 3A enzymes. Using the extended clearance model, through simulations, we identified the ratio of sinusoidal efflux clearance (CL) over the sum of metabolic and biliary CLs as important in predicting the impact of HI on the AUC of dual OATP/CYP3A substrates. Because HI may reduce hepatic CYP3A-mediated CL to a greater extent than biliary efflux CL, the greater the contribution of the former versus the latter, the greater the impact of HI on drug AUC ratio (AUC_{HI}). Using physiologically-based pharmacokinetic modeling and simulation, we predicted relatively well the AUC_{HI} of OATP substrates that are not significantly metabolized (pitavastatin, rosuvastatin, valsartan, and gadoxetic acid). However, there was a trend toward underprediction of the AUC_{HI} of the dual OATP/CYP3A4 substrates fimasartan and atorvastatin. These predictions improved when the sinusoidal efflux CL of these two drugs was increased in healthy volunteers (i.e., before incorporating the effect of HI), and by modifying the directionality of its modulation by HI (i.e., increase or decrease). To accurately predict the effect of HI on AUC of hepatobiliary cleared drugs it is important to accurately predict all hepatobiliary pathways, including sinusoidal efflux CL.

Study Highlights

WHAT IS THE CURRENT KNOWLEDGE ON THE TOPIC?

Hepatic impairment (HI) affects the systemic exposure of drugs that are OATP/CYP3A4 substrates (area under the plasma concentration–time curve [AUC])

This is an open access article under the terms of the [Creative Commons Attribution-NonCommercial](https://creativecommons.org/licenses/by-nc/4.0/) License, which permits use, distribution and reproduction in any medium, provided the original work is properly cited and is not used for commercial purposes.

© 2023 The Authors. *CPT: Pharmacometrics & Systems Pharmacology* published by Wiley Periodicals LLC on behalf of American Society for Clinical Pharmacology and Therapeutics.

increasing >10-fold) to a greater extent than those drugs that are substrates of OATP/biliary efflux transporters (AUC increasing <5-fold).

WHAT QUESTION DID THIS STUDY ADDRESS?

Why does HI affect the systemic exposure of dual OATP/CYP3A4 substrates greater than those that are transported by OATP/biliary efflux transporters? Can this difference be predicted by physiologically-based pharmacokinetic modeling and simulation?

WHAT DOES THIS STUDY ADD TO OUR KNOWLEDGE?

Using the extended clearance (CL) model, we highlighted factors that drive the increase in HI in the blood AUC of OATP/CYP3A4 versus OATP/biliary efflux transporter substrates. We showed that accurate estimation of all hepatobiliary CLs, including the often-overlooked sinusoidal efflux CL, and their modulation in HI, are critical factors to improve predictions of pharmacokinetic changes of drugs in HI.

HOW MIGHT THIS CHANGE DRUG DISCOVERY, DEVELOPMENT, AND/OR THERAPEUTICS?

By better understanding what drives pharmacokinetic changes of OATP/CYP3A substrate drugs in HI, we can better predict the effect of HI on their systemic exposure.

INTRODUCTION

Hepatic impairment (HI) affects the pharmacokinetics (PKs) of drugs through physiological changes, such as modulation of drug metabolizing enzyme and transporter (DMET) abundance, reduction of liver functional volume, reduction in drug-binding protein concentration and hematocrit, and modulation of mesenteric and hepatic (arterial and portal) blood flows.^{1–5} These changes often result in increased systemic exposure (i.e., the area under the plasma concentration–time curve [AUC]) of drugs, which can impact their safety profile. Therefore, regulatory agencies recommend that the PKs of drugs that are hepatically cleared should be assessed in people with HI to inform dose-adjustment in these subjects.^{6,7}

Physiologically-based PK modeling and simulation (PBPK M&S) is a promising approach to assess the impact of HI on drug PKs,^{4,8–10} and can either replace or supplement PK studies in HI or inform PK study design in HI to avoid adverse drug reactions. However, before using such PBPK models with confidence, their prediction performance in HI needs to be assessed. Whereas PBPK M&S studies assessing the effect of HI on drugs that are metabolized by cytochromes P450 (CYP) are available,^{10,11} there are limited data on the predictive performance of such models for drugs that are substrates of hepatic drug transporters, such as the sinusoidal organic anion transporting polypeptides (OATPs) and the ABC efflux transporters, such as P-glycoprotein (P-gp), Breast Cancer Resistance

Protein (BCRP), or multidrug resistance proteins 2, 3, or 4 (MRP2/3/4).¹² These transporters, as well as hepatic metabolism, can affect the systemic exposure and response of many drugs, including cholesterol-lowering (e.g., HMG-CoA reductase inhibitors), antihypertensive (e.g., angiotensin II receptor blockers), antiviral (e.g., NS3/4A protease inhibitors), and antidiabetic (e.g., meglitinides) drugs.^{13–15}

Interestingly, the AUC of drugs that are OATP substrates and significantly metabolized, in particular by cytochrome P450 (CYP) 3A enzymes, can increase significantly (as much as 32-fold) in patients with HI (Table 1). This increase in AUC increases with the degree of HI, classified as the Child-Pugh (CP) score CP-A (mild), CP-B (moderate), or CP-C (severe; Table 1). In contrast, the AUC of OATP and biliary efflux transporter (BET) substrates, that are not significantly metabolized and mostly excreted unchanged in the urine and/or bile, such as pitavastatin, rosuvastatin, valsartan, pravastatin, and gadoxetic acid, are less affected by HI (<5-fold; Table 1). The reason for this difference needs to be elucidated to successfully predict, through PBPK M&S, the impact of HI on the AUC of drugs that are OATP/BET or OATP/CYP3A substrates. To note, in this paper, we refer to OATP/BET substrates as OATP substrates whose hepatic elimination is primarily mediated by biliary excretion of the unchanged drug and OATP/CYP3A4 (we recognize that these drugs may also be metabolized by CYP3A5, but for simplicity we refer to only CYP3A4) substrates as OATP substrates whose hepatic elimination is mediated by CYP3A4-mediated metabolism (even though they may also be partially eliminated by BET).

TABLE 1 Effect of different degrees of HI on the plasma AUC of OATP substrate drugs as well as their major route of elimination.

Drug	AUCR _{HI} (CP-A)	AUCR _{HI} (CP-B)	AUCR _{HI} (CP-C)	Uptake transport (liver)	Efflux transport (liver)	Metabolism	Major elimination route
Asunaprevir	0.79	9.83	32.1	OATP1B1, OATP2B1	P-gp	CYP3A	Metabolism + biliary excretion
Glecaprevir	1.15	1.89	15.8	OATP1B1/3	BCRP, P-gp	CYP3A	Biliary excretion
Grazoprevir	1.66	4.82	11.7	OATP1B1	BCRP, P-gp	CYP3A	Biliary excretion
Paritaprevir	0.72	2.05	9.84	OATP1B1/3	BCRP, P-gp	CYP3A	Metabolism
Atorvastatin	4.4	9.8	–	OATP1B1/3, OATP2B1, NTCP	BCRP, P-gp, MRP2 ^c , MRP3, MRP4 ^c	CYP3A, minor: UGT	Metabolism
Elagolix	0.98	3.04	6.83	OATP1B1	P-gp	CYP3A4 (major), CYP2D6, CYP2C8, UGT (minor)	Metabolism
Voxilaprevir	–	4.49	6.25	OATP1B1/3	BCRP, P-gp	CYP3A4 (major), CYP2C8, CYP1A2	Biliary excretion
Fimasartan	1.11	5.17	–	OATP1B1, OATP2B1	BCRP	CYP3A4 (major), UGT1A3, UGT1A1, UGT	Biliary excretion
Repaglinide	–	4.3 ^a	4.3 ^a	OATP1B1, OATP1B3 ^c	P-gp ^c	CYP2C8, CYP3A, minor: UGT	Metabolism
Pitavastatin	1.28	3.54	–	OATP1B1/3, OATP2B1, NTCP	BCRP, P-gp, MRP3 ^c , MRP4 ^c	Minimal ^d : UGT2B7, CYP2C9	Biliary excretion
Valsartan	2.21	2.14	–	OATP1B1/3, OATP2B1 ^c	MRP2, P-gp ^c	Minimal ^d : CYP2C9	Biliary excretion
Gadoxetic acid (i.v.)	1.58	1.31	1.62	OATP1B1/3, NTCP	MRP2	Minimal ^d	Biliary + renal excretion
Pravastatin	1.34 ^b	1.34 ^b	1.34 ^b	OATP1B1/3, OATP2B1, NTCP	MRP2, MRP3 ^c , MRP4 ^c , BCRP ^c	Minimal ^d : CYP3A, UGT	Biliary excretion
Rosuvastatin	1.05	1.21	–	OATP1B1/3, NTCP, OATP2B1	BCRP, MRP2, P-gp, MRP3 ^c	Minimal ^d : CYP2C9, CYP2C19, CYP3A, UGT	Biliary (major) + renal excretion

Note: Data were retrieved from the University of Washington Drug Interaction Database (DIDB) (<http://www.druginteractionsolutions.org>; last accessed August 2023). See Appendix S1 for a full list of references for each drug. Hepatic impairment studies were conducted in populations consisting of mainly (>80%) White subjects, except for pitavastatin and fimasartan, which were conducted primarily in Asian subjects. *SLCO1B1* genotype information was not provided.

Abbreviations: AUCR_{HI}, ratio of drug area under the concentration–time curve in HI vs. healthy; CP, Child–Pugh; HI, hepatic impairment; NA, not available.

^aMixed CP-B and CP-C populations.

^bCP score not reported.

^cConflicting data for the involvement of the indicated pathway (e.g., different *in vitro* systems provide different conclusions); further investigation is needed to confirm contribution.

^dMinimal metabolism was concluded by the absence of significant clinical drug–drug interaction (AUC ratio < 20%) with known inhibitors of the involved pathways.

The aims of this study were three-fold: (1) to understand the key factors that can affect the increase in HI of AUC of the dual OATP/BET or OATP/CYP3A4 substrates using the extended clearance model; (2) to assess the performance of PBPK models (using Simcyp, Certara, NJ) to predict the changes in AUC of OATP/BET substrates (pitavastatin, rosuvastatin, valsartan, and gadoxetic acid) or OATP/CYP3A4 substrates (atorvastatin and fimasartan) for various degrees of HI (CP-A to C); and (3) to use the insights gained from 1 above to improve PBPK model predictions of the effect of HI on the systemic exposure of OATP/CYP3A4 substrates using atorvastatin and fimasartan as test drugs.

METHODS

Systemic exposure of hepatically transported drugs after intravenous administration

The extended clearance (CL) model stipulates that all hepatobiliary CLs (uptake, efflux, and metabolism), in addition to hepatic blood flow (Q_H), and the unbound fraction in blood ($f_{u,b}$) determine hepatic drug CL (CL_H).^{16–19} Here, we have deliberately chosen to quantify the change in unbound blood AUC (AUC_u) in HI, rather than total blood or plasma AUC, as it is the unbound blood concentration that drives drug efficacy and toxicity.

When a transported drug is predominately eliminated hepatically (i.e., negligible renal or intestinal excretion), its AUC_u following i.v. dosing is defined as follows (derived from ref. 19):

$$\frac{AUC_u}{\text{Dose (IV)}} = \frac{f_{u,b}}{Q_H} + \frac{1}{CL_{in}^s} \cdot \left(1 + \frac{CL_{ef}^s}{CL_{met} + CL_{ef}^c} \right) \quad (1)$$

where CL_{in}^s is the intrinsic sinusoidal influx CL, CL_{ef}^s is the intrinsic sinusoidal efflux CL, CL_{met} is the intrinsic metabolic CL, and CL_{ef}^c is the intrinsic canalicular efflux CL. Here, the CL_{in}^s , CL_{ef}^s , and CL_{ef}^c include both active transport and passive diffusion.

When $CL_{ef}^s \ll CL_{met} + CL_{ef}^c$, AUC_u is a function of $f_{u,b}$, Q_H , and CL_{in}^s only, as follows:

$$\frac{AUC_u}{\text{Dose (IV)}} = \frac{f_{u,b} \cdot CL_{in}^s + Q_H}{Q_H \cdot CL_{in}^s} \quad (2)$$

In this case, the hepatic uptake is the rate-determining step (RDS) of the drug hepatic CL (scenario referred here as $RDS_{CL,H} = \text{uptake}$).

Systemic exposure of transported drugs after oral administration

For oral administration, according to the extended clearance model, the AUC_u of a drug predominately eliminated hepatically is described as follows (derived from ref. 19):

$$\frac{AUC_u}{\text{Dose (PO)}} = f_a \cdot F_G \cdot \frac{1}{CL_{in}^s} \cdot \left(1 + \frac{CL_{ef}^s}{CL_{met} + CL_{ef}^c} \right) \quad (3)$$

Therefore, the blood AUC_u of drugs administered p.o. is affected by changes in f_a , F_G , and in CL_{in}^s , as well as changes in the ratio $CL_{ef}^s / (CL_{met} + CL_{ef}^c)$. Note, for oral administration, Q_H is not a determinant of drug blood AUC_u .

When $CL_{ef}^s \ll CL_{met} + CL_{ef}^c$ (i.e., $RDS_{CL,H} = \text{uptake}$):

$$\frac{AUC_u}{\text{Dose (PO)}} = \frac{f_a \cdot F_G}{CL_{in}^s} \quad (4)$$

F_G can be estimated from the villi blood flow (Q_{villi}), gut metabolism, and drug permeability in the gastrointestinal tract, as described before²⁰:

$$F_G = \frac{Q_{villi}}{Q_{villi} + f_{u,G} \cdot CL_{met,G} \cdot \left(1 + \frac{Q_{villi}}{CL_{perm}} \right)} \quad (5)$$

$f_{u,G}$ is the unbound drug fraction in the enterocytes, $CL_{met,G}$ is the intrinsic metabolic CL in the gut, and CL_{perm} is the drug intestinal permeability.

Simulation of the effect of CP-C on the exposure of transported virtual compounds administered i.v.

First, we illustrate the importance of the ratio $CL_{ef}^s / (CL_{met} + CL_{ef}^c)$ (which determines the RDS of CL_H) on the effect of HI on the AUC_u of i.v. administered drugs. The i.v. administration was chosen to focus on hepatic (vs. gut) drug CL. We created virtual compounds with fixed hepatic intrinsic CLs ($CL_{int,H}$) of 100, 1000, and 10,000 mL/min, corresponding to low hepatic extraction ($E_H = 6\%$), intermediate E_H (37%), and high E_H (86%), where $CL_{int,H}$ is a function of all hepatobiliary intrinsic CLs:

$$CL_{int,H} = \frac{CL_{in}^s \cdot (CL_{met} + CL_{ef}^c)}{CL_{ef}^s + CL_{met} + CL_{ef}^c} \quad (6)$$

Different E_H were examined because Equation 1 suggests that hepatic blood flow is a determinant of the blood AUC of i.v.-administered drugs.

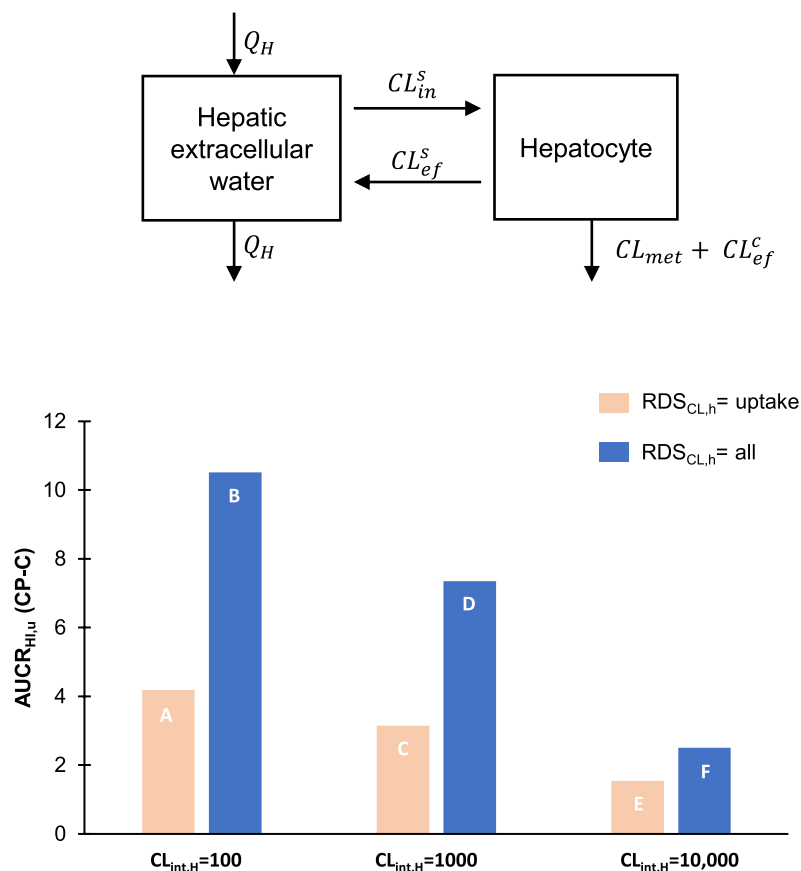


FIGURE 1 After i.v. administration, both the rate-determining step of hepatic clearance and the hepatic extraction ratio affect the magnitude of the effect of hepatic impairment on the blood unbound AUC of the transported drugs. All clearance units are in mL/min. $AUCR_{HI,u}$, ratio of area under the blood unbound concentration–time profile in hepatic impaired subjects vs. healthy volunteers; $CL_{int,H}$, intrinsic hepatic clearance; CL_{met} , intrinsic metabolic clearance; CL_{ef}^c , intrinsic canalicular efflux clearance; CL_{ef}^s , intrinsic sinusoidal efflux clearance; CL_{in}^s , intrinsic sinusoidal influx clearance; $RDS_{CL,H}$, rate-determining step of hepatic clearance (CL_H).

	$CL_{int,H}$	CL_H	E_H (%)	$RDS_{CL,H}$	CL_{in}^s	CL_{ef}^s	$CL_{met} + CL_{ef}^c$	$CL_{ef}^s / (CL_{met} + CL_{ef}^c)$	CL_{in}^s / CL_{ef}^s
A	100	94	6	Uptake	102	1	50	0.02	102
B				All	1000	500	55.5	9	2
C	1000	628	37	Uptake	1020	10	500	0.02	102
D				All	10,000	5000	555	9	2
E	10,000	1445	86	Uptake	10,200	100	5000	0.02	102
F				All	100,000	50,000	5555	9	2

For each level of E_H (see Figure 1 for details), two scenarios of the rate-determining step of CL_H were investigated: $RDS_{CL,H} = \text{uptake}$ (i.e., $CL_{ef}^s \ll CL_{met} + CL_{ef}^c$), and $RDS_{CL,H} = \text{all}$ (i.e., condition $CL_{ef}^s \ll CL_{met} + CL_{ef}^c$ does not apply and CL_H is determined by all hepatobiliary CLs). The ratios $CL_{ef}^s / (CL_{met} + CL_{ef}^c)$ and CL_{in}^s / CL_{ef}^s were kept the same for compounds A, C, and E, for which $RDS_{CL,H} = \text{uptake}$ (0.02 and 102, respectively), and for compounds B, D, and F, for which $RDS_{CL,H} = \text{all}$ (9 and 2, respectively); those ratios were chosen arbitrarily to satisfy the different $RDS_{CL,H}$ scenarios for given $CL_{int,H}$ values.

For these virtual compounds, we assumed that: (1) renal elimination was negligible; (2) CL_{in}^s was mediated via OATP1B1 ($CL_{int,OATP1B1} = 95\%$ of CL_{in}^s) and passive diffusion ($CL_{int,pd} = 5\%$ of CL_{in}^s); (3) CL_{ef}^s was mediated by passive diffusion only (no active transport, i.e., $CL_{ef}^s = CL_{int,pd}$); (4) $CL_{met} + CL_{ef}^c$ was mediated by CYP3A4 metabolism ($CL_{int,CYP3A4} = 90\%$ of

$CL_{met} + CL_{ef}^c$), CYP2C9 metabolism ($CL_{int,CYP2C9} = 5\%$ of $CL_{met} + CL_{ef}^c$), and P-gp canalicular efflux ($CL_{int,P-gp} = 5\%$ of $CL_{met} + CL_{ef}^c$); (5) $f_{u,b}$ was equal to 1 and unaffected in HI. A summary of physiological parameters and incorporated changes in HI is described in Table S1. Briefly, relevant PK parameters were modulated in CP-C as follows (from the most affected to the least affected): $CL_{int,CYP3A4}$ (−85%), $CL_{int,OATP1B1}$ (−77%), $CL_{int,P-gp}$ (−75%), $CL_{int,CYP2C9}$ (−73%), $CL_{int,pd}$ (−56%), and Q_H (−6%). Note that for DMETs, the changes described above reflect the modulation of DMET abundance (if any) at the cellular level (i.e., DMET abundance in pmol per million cells or per mg of microsomal protein) and functional liver weight in HI, whereas for passive diffusion, the change reported is explained by the reduction of the functional liver weight. Note, we assumed that the enzyme/transporter activity per pmol of enzyme/transporter did not change between healthy volunteers and those with HI. The changes described above are based

on the Simcyp version 21 healthy volunteers (HVs) and CP-C population representatives, that is, the individual that represents the features of the majority part of a given population.²¹

The drugs' AUC_u in the CP-C population was calculated using Equation 1 and changes in Q_H , passive diffusion, and DMET abundance described above and in Table S1. AUCR_{HI,u} was calculated as the ratio of AUC_u in patients with HI versus HVs. We chose to simulate AUCR_{HI,u} in the CP-C population as it is associated with the greatest effect in HI.

Simulation of the effect of CP-C on the exposure of Compound X, a model OATP/CYP3A4 drug administered p.o.

In the second set of simulations, we predicted the AUCR_{HI,u} after p.o. administration of a model OATP/CYP3A4 drug, named "Compound X" (modeled on atorvastatin; Table 2). CL_{int,H} was calculated (Equation 6) assuming that the hepatic uptake was mediated 95% by OATP1B1 and 5% by passive diffusion, sinusoidal efflux was mediated only by passive diffusion, metabolism was 100% via CYP3A4, and canalicular efflux CL was 100% via P-gp, with negligible renal excretion. CL_{met,g} was estimated from the hepatic CL_{met} using the ratio of the abundance of CYP3A4 in the gut and the liver in the HVs ("Sim-Healthy Volunteers") population of Simcyp

version 21 (Table S1). The $f_a \cdot F_G$ was estimated from Equation 5, where $f_a = 1$ (mediated only by passive diffusion), $f_{u,G} = 1$ and CL_{perm} = 1.16 mL/min/kg (calculated from the effective intestinal permeability in atorvastatin library compound of Simcyp version 21 [Table S6], as previously described²⁰).

To predict AUCR_{HI,u} of Compound X in CP-C, we incorporated changes in hepatic passive diffusion, OATP1B1, and P-gp transport, hepatic CYP3A4 metabolism described above and in Table S1. Gut CYP3A4-mediated CL_{int} (−52%) and Q_{villi} (+100%) in CP-C were also modulated (Table S1). We assumed that CL_{perm} was not affected in HI.

Sensitivity analyses of the ratio $CL_{ef}^s / (CL_{met} + CL_{ef}^c)$ on the AUCR_{HI,u} of compound X

To analyze the effect of varying the ratio $CL_{ef}^s / (CL_{met} + CL_{ef}^c)$ (and consequently, the different RDS_{CL,H} scenarios) on the simulated AUCR_{HI,u} in CP-C of Compound X, we performed sensitivity analyses of AUCR_{HI,u} by scaling either CL_{ef}^s or CL_{met} (and therefore CL_{met,G}; derived from CL_{met,H}) in HVs (i.e., before incorporating the effect of CP-C) by a factor of 0.001 to 1000 while keeping the other hepatobiliary CLs the same as in the initial model (Table 2). No sensitivity analysis for CL_{ef}^c was performed as this was a minor

TABLE 2 Simulated effect of hepatic impairment on the unbound blood exposure (AUCR_{HI,u}) of Compound X.

Parameter	Initial value (HVs)	Simulated value in CP-C	Simulated change in CP-C
CL _{in} ^s	405	96	−76%
CL _{ef} ^s	25	11	−56%
CL _{met}	58	8.5	−85%
CL _{ef} ^c	4.3	1.1	−75%
CL _{int,h}	290	45	−85%
$CL_{ef}^s / (CL_{met} + CL_{ef}^c)$	0.40 ^a	1.1	+188%
$1 + CL_{ef}^s / (CL_{met} + CL_{ef}^c)$	1.40	2.1	+43%
$CL_{met} / (CL_{met} + CL_{ef}^c)$	0.93	0.89	−5%
CL _{met,g}	0.42	0.20	−52%
$f_a \cdot F_g$	0.69	0.84	+21%
AUCR _{HI,u} (CP-C)	–	7.84	–

Note: Initial values of CL_{in}^s, CL_{ef}^s, CL_{met}, and CL_{ef}^c were obtained from atorvastatin in vitro in vivo extrapolation of hepatic CL.^{34,35} The units of all CLs in this table are in mL/min/kg body weight.

Abbreviations: AUCR_{HI,u}, ratio of unbound blood AUC in HI versus healthy; CL_{ef}^c, intrinsic canalicular efflux clearance; CL_{int,h}, intrinsic hepatic clearance; CL_{met}, intrinsic hepatic metabolic clearance; CL_{met,g}, intrinsic gut metabolic clearance; CL_{in}^s, intrinsic hepatic influx clearance; CP-C, Child-Pugh C; F_g , fraction escaping gut metabolism; HVs, healthy volunteers.

^aCL_{ef}^s / (CL_{met} + CL_{ef}^c) = 0.40 suggests that the hepatic clearance is rate-determined by all hepatic clearances rather than uptake only.³⁵

(<10%) elimination pathway of Compound X (Table 2). The effects of CP-C on all physiological parameters ($f_{u,b}$, DMET abundance, and blood flows) were kept the same as described above.

Our research group previously reported a 38% increase in the abundance of MRP3 in cirrhosis.² Therefore, assuming that Compound X's sinusoidal efflux is 90% mediated by MRP3 and 10% passive diffusion (vs. by passive diffusion only in earlier simulations), we performed similar sensitivity analyses, as described above, but using this reported increase in MRP3 abundance in cirrhosis.

Prediction of the effect of HI on the systemic PKs of OATP/BET and OATP/CYP3A4 substrates using PBPK M&S

The effect of CP-A, CP-B, and CP-C on the plasma AUC of four OATP/BET substrates (pitavastatin, rosuvastatin, valsartan, and gadoxetic acid) and two dual OATP/CYP3A4 substrates (atorvastatin and fimasartan) was simulated in Simcyp version 21. These drugs were chosen because they are all OATP substrates and either had available PBPK models on Simcyp version 21 (valsartan and atorvastatin) or had i.v. PK data that could be used to develop new PBPK models (pitavastatin, rosuvastatin, gadoxetic acid, and fimasartan; see Appendix S1). For all these compounds, a full PBPK distribution model with the permeability-limited liver model was used. All models were validated by comparing the simulated and

observed PK profiles from three to six studies, including the HV controls of the HI studies, where available (Figures S1–S6). This validation was not comprehensive as it did not include drug–drug interaction studies, tissue imaging studies, genotype differences, or metabolites/excreta data. These studies used for model validations were distinct from those used for model development and optimization.

We then simulated the drugs' AUC_{HI} (i.e., the plasma AUC in HI vs. HVs) in CP-A, CP-B, and, for gadoxetic acid, CP-C (data in CP-C were not available for other drugs), and compared them with reported data^{22–27} (see Table S8 for trial design and demographic information). Note, we simulated the effect of HI on plasma AUC rather than AUC_u because the measured concentrations in HI trials used for validation were total and not unbound plasma (or, in the case of gadoxetic acid, serum) concentrations. Two types of simulations of the effect of HI were conducted: first, using Simcyp cirrhosis populations (“Sim-cirrhosis CP-A,” “Sim-cirrhosis CP-B,” and “Sim-cirrhosis CP-C”) without incorporating changes in transporter abundance at the cellular level (i.e., abundance in pmol/million hepatocytes) but including the change in the functional liver volume (tissue volume fold-scalar in the Tissue Composition Tab, reported in Table 3); second, with transporter abundance changes at the cellular level (this was done by applying transporter abundance changes reported in Table 3 [based on Simcyp version 21 cirrhosis population files]). Physiological changes, other than transporter abundance and tissue volume scalar, were kept the same as those in the population library in Simcyp simulator

TABLE 3 Changes in hepatic transporter abundance and functional volume incorporated in PBPK model predictions of the effect of hepatic impairment on the systemic exposure of transported drugs.

	Ratio CP-A vs. HVs	Ratio CP-B vs. HVs	Ratio CP-C vs. HVs
Hepatic transporter abundance (pmol/million hepatocytes)			
NTCP	1	1	1
OATP1B1	1	0.81	0.52
OATP1B3	0.81	0.45	0.28
OATP2B1	1	1	1
MRP3	1	1	1
P-gp	0.57	0.57	0.57
MRP2	0.69	0.73	0.73
BCRP	1	1	1
Hepatocellularity (million hepatocytes/g of liver)			
Liver volume (L)	0.86	0.71	0.59
Liver density (g/L)	1	1	1

Note: Data based on “Sim-Healthy Volunteers” (HVs), “Sim-Cirrhosis CP-A,” “Sim-Cirrhosis CP-B,” and “Sim-Cirrhosis CP-C” populations in Simcyp version 21.

Abbreviations: CP, Child-Pugh; PBPK, physiologically-based pharmacokinetic.

version 21. Population-specific physiological parameters are summarized elsewhere.¹¹ Root mean square error and mean error were used to compare performances in terms of precision and bias, respectively.

Sensitivity analyses of CL_{ef}^s values of atorvastatin and fimasartan on $AUCR_{HI}$ in moderate HI (CP-B)

To optimize predictions of $AUCR_{HI}$ in CP-B for atorvastatin and fimasartan, we increased the CL_{ef}^s in both compound files (initially assumed to be equal to passive diffusion for atorvastatin and negligible for fimasartan) up to 10,000-fold and observed the resulting effect on $AUCR_{HI}$. Negligible CL_{ef}^s was assumed in the initial fimasartan model to estimate CL_{in}^s from i.v. clinical data (assuming $RDS_{CL,H}$ = uptake) because data on passive diffusion and hepatobiliary CLs of the drug are not available. For these simulations, the transporter abundance changes at the cellular level were included (Table 3). Additionally, we performed the same sensitivity analyses but arbitrarily assumed that 90% of the sinusoidal efflux was mediated by MRP3 (vs. passive diffusion only) and incorporated our previous data on MRP3 modulation by cirrhosis (+38%; described above).

RESULTS

The $RDS_{CL,H}$ and the hepatic extraction of a drug determine the magnitude of $AUCR_{HI,u}$ after i.v. administration

Simulations of different scenarios of $RDS_{CL,H}$ and E_H for i.v. administration show that $AUCR_{HI,u}$ is greater when $RDS_{CL,H}$ = all than when $RDS_{CL,H}$ = uptake (e.g., B vs. A, D vs. C, and F vs. E in Figure 1). This is because for the former ($RDS_{CL,H}$ = all), the AUC_u in HI is determined by changes in CL_{in}^s , $CL_{ef}^s / (CL_{met} + CL_{ef}^c)$, and Q_H (note that here, for simplicity, $f_{u,b}$ was assumed to equal 1; Equation 1). In contrast, when $RDS_{CL,H}$ = uptake (i.e., $CL_{ef}^s \ll CL_{met} + CL_{ef}^c$ as in A, C, and E), the modulation of the ratio $CL_{ef}^s / (CL_{met} + CL_{ef}^c)$ in HI (e.g., reduced CYP3A4 or biliary CL) should not affect the AUC_u of the drug (Equation 2).¹⁷

In addition, irrespective of the $RDS_{CL,H}$, as E_H increases toward 100% (i.e., as E_H approaches hepatic blood flow), $AUCR_{HI,u}$ diminishes. Indeed, HI has little effect on Q_H (Table S1). Therefore, for i.v. administration, the $AUCR_{HI,u}$ is higher for low E_H drugs (where CL_H is highly dependent on $CL_{int,H}$) than for high E_H drugs (where CL_H is highly dependent on Q_H).

The ratio $CL_{ef}^s / (CL_{met} + CL_{ef}^c)$ and $f_a \cdot F_G$ are major determinants of $AUCR_{HI,u}$ of orally administered drugs

In the case of p.o. administration, when $RDS_{CL,H}$ = all, $AUCR_{HI,u}$ is affected by changes in CL_{in}^s , the ratio $CL_{ef}^s / (CL_{met} + CL_{ef}^c)$, and $f_a \cdot F_G$ (Equation 3).

The simulated $AUCR_{HI,u}$ of Compound X in CP-C is 7.84 (Table 2). Through sensitivity analyses, we determined whether changes in CL_{ef}^s or CL_{met} could affect Compound X's $AUCR_{HI,u}$ (Figure 2). Note that Figure 2a,c show simulations where sinusoidal efflux is assumed to be mediated by passive diffusion (which decreases in HI due to change in liver functional volume), whereas Figure 2b,d show simulations where sinusoidal efflux is assumed to be mediated by MRP3 (fraction transported f_t = 90%) and where MRP3 abundance in HI increases by 38%.²

We found that $AUCR_{HI,u}$ was sensitive to variation in CL_{ef}^s (Figure 2a,b), and could be as large as 45 for Compound X (Figure 2b). This is because, as CL_{ef}^s increases (in the HV model, using the diamond as a reference point), drug CL_H become more dependent on hepatic elimination (i.e., $CL_{met} + CL_{ef}^c$) than on hepatic uptake (CL_{in}^s); when CYP3A4-mediated CL_{met} is the main contributor to hepatic elimination, this results in a large $AUCR_{HI,u}$ because this parameter is more affected by HI than CL_{in}^s . In contrast, as CL_{ef}^s decreases, $AUCR_{HI,u}$ decreases because CL_H becomes rate-determined by uptake only, and any modulation of CL_{ef}^s , CL_{met} , and/or CL_{ef}^c by HI does not affect drug AUC_u .

The relationship between CL_{met} and $AUCR_{HI,u}$ is less straightforward (Figure 2c,d). Indeed, the extent of metabolism (i.e., CL_{met} value) affects not only the $RDS_{CL,H}$, but also gut availability (i.e., $f_a \cdot F_G$). In Figure 2c, decreasing CL_{met} (using the diamond as a reference point) results first in a slight increase in the predicted $AUCR_{HI,u}$ because hepatic elimination decreases. However, as CL_{met} continues to decrease, hepatic elimination becomes driven by canalicular efflux rather than metabolism (note that in the initial model, hepatic elimination was 93% driven by metabolism; Table 2). Because the abundance of canalicular efflux transporters is less affected by HI than the abundance of CYP3A4 (Table S1;^{1,2}), $AUCR_{HI,u}$ is lower when hepatic elimination is mediated by canalicular efflux rather than metabolism. These opposite effects are reflected by the dash-dotted purple line in Figure 2c,d, showing a bump around the initial prediction. In addition, as the extent of metabolism (in both the liver and the gut; gut metabolism was estimated based on hepatic metabolism and the relative CYP3A4 abundance in gut vs. liver) decreases, more drug escapes intestinal metabolism (i.e., $f_a \cdot F_G$ increases, getting closer to 1, and therefore less affected by HI; see dotted blue line in Figure 2c,d). Increasing CL_{met} had the

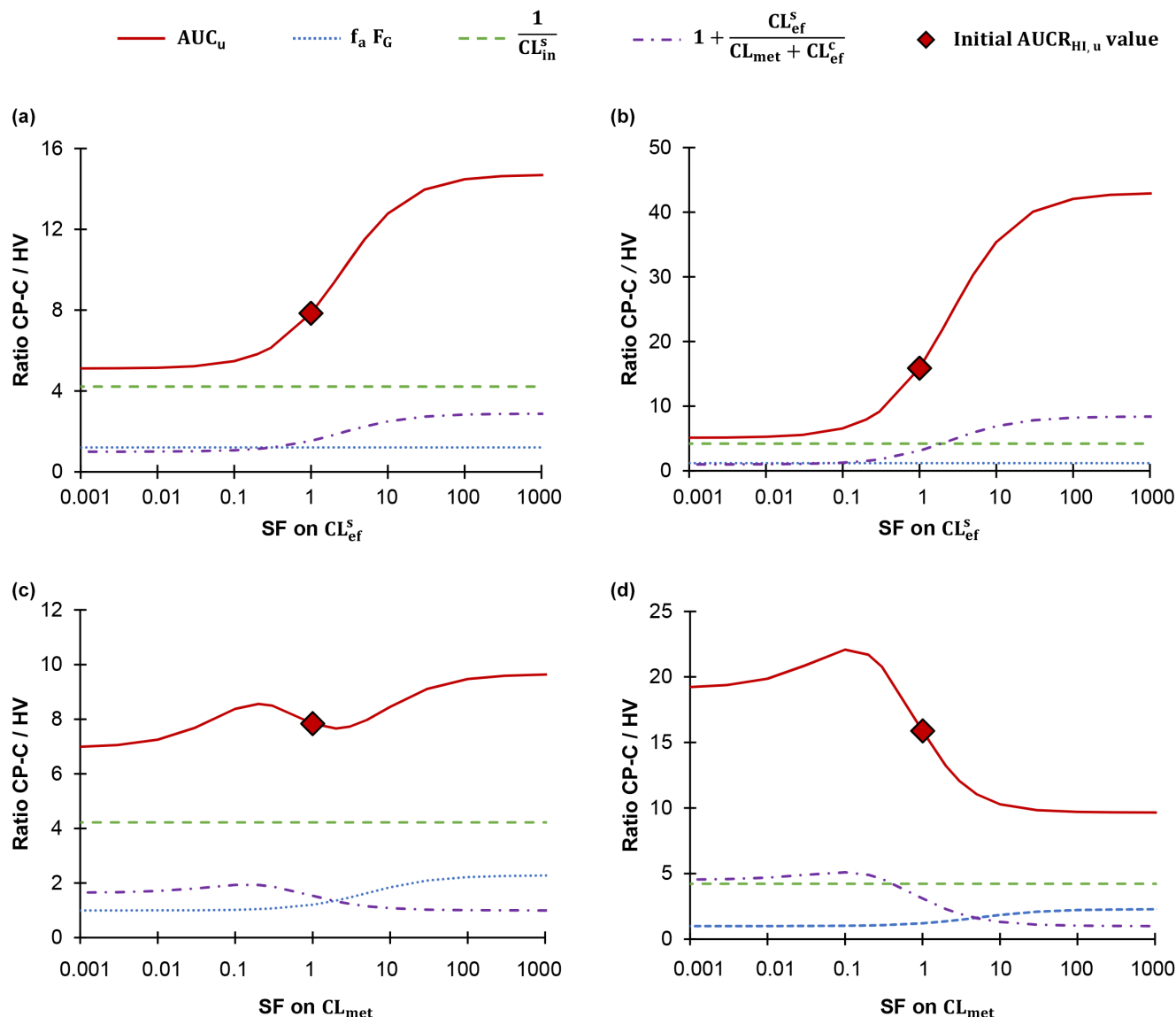


FIGURE 2 Both the sinusoidal efflux CL and hepatic plus intestinal metabolic CL affect the magnitude of the $AUCR_{HI,u}$ of orally administered transported drugs. For panels (a, c), drug sinusoidal efflux was assumed to be passive (and decreasing in HI as a result of loss of functional liver volume; see Table 3), whereas for panels (b, d), 90% of the drug was assumed to be transported across the sinusoidal membrane by MRP3, and the abundance of MRP3 in CP-C was assumed to increase by 38%, based on our proteomic data.² The effect of CP-C on each component of Equation 3 are also shown, that is, gut availability (dotted blue lines), intrinsic hepatic influx (dashed green lines) and sinusoidal efflux relative to hepatic elimination (metabolism and canalicular efflux; dash-dotted purple lines). $AUCR_{HI,u}$ (shown as a continuous red lines) is the product of the ratio of each of these three components in CP-C vs. HVs (i.e., the continuous red lines are the products of the other three lines). AUC_u , area under the blood unbound concentration–time profile; $AUCR_{HI,u}$, ratio of blood unbound AUC in hepatic impairment vs. healthy volunteers; CL_{met} , intrinsic metabolic clearance; CL_{ef}^c , intrinsic canalicular efflux clearance; CL_{ef}^s , intrinsic sinusoidal efflux clearance; CL_{in}^s , intrinsic sinusoidal influx clearance; CP, Child-Pugh; f_a , fraction of the administered drug absorbed in enterocytes; F_G , fraction of the drug escaping gut metabolism; HV, healthy volunteers.

opposite effect: as CL_{met} increases, the $RDS_{CL,H}$ becomes uptake (dash-dotted purple line in Figure 2c,d), but intestinal availability ($f_a \cdot F_G$) becomes more vulnerable to the decrease in intestinal CYP3A4 abundance in HI (dotted blue line in Figure 2c,d).

We found that the predicted $AUCR_{HI,u}$ were higher when we assumed that CL_{ef}^s was mediated by active transport (MRP3, $f_t = 90\%$), which might increase in HI² (see discussion for conflicting data) than when we assumed that CL_{ef}^s was mediated by passive diffusion,

which decreases in HI as a result of the loss of functional liver volume (Figure 2b vs. Figure 2a and Figure 2d vs. Figure 2c).

Note that we simulated here the effect of HI on the blood unbound AUC, because unbound concentrations (rather than total) drive efficacy and toxicity. In other words, we did not incorporate the effect of HI on drug binding to plasma proteins (i.e., $f_{u,b}$). Should we have considered the total (bound + unbound) blood AUC, the effect of HI would have been smaller, because $f_{u,b}$ generally increases in HI due to a decrease in the abundance of drug binding plasma proteins.^{5,28}

The $AUCR_{HI}$ of OATP/BET substrates were relatively well predicted by PBPK M&S

Using PBPK M&S, we predicted the $AUCR_{HI}$ of OATP/BET substrates pitavastatin, rosuvastatin, valsartan, and gadoxetic acid within two-fold of the observed data (Figure 3; Figures S7 and S8). Predictions were modestly improved (reduced root mean square error and mean error) when accounting for hepatic transporter abundance changes in addition to changes in functional liver volume in HI (Figure 3b) versus accounting only for changes in functional liver volume (Figure 3a).

The $AUCR_{HI}$ of the OATP/CYP3A4 substrates atorvastatin and fimasartan were relatively well-predicted by PBPK M&S, but these predictions improved when $CL_{int,s,ef}^s$ was increased

$AUCR_{HI}$ for dual OATP/CYP3A4 substrates atorvastatin (in both CP-A and CP-B) and fimasartan (in CP-B) were predicted within two-fold of the observed values, but, except for fimasartan in CP-A, fell below the 0.8 to 1.25-fold bioequivalence range (Figure 4a,b; Figures S7 and S8). Therefore, based on the outcome of the sensitivity analyses discussed above, we hypothesized that an increase in the CL_{ef}^s values of the two drugs would move the predicted $AUCR_{HI}$ into the bioequivalence range. Indeed, the $AUCR_{HI}$ of the two drugs fell within the bioequivalence range when we assumed that CL_{ef}^s was increased (rather than decreased) in HI (Figure 4c,d).

DISCUSSION

The systemic exposure of drugs that are OATP substrates increases significantly in HI. Whereas the $AUCR_{HI}$ in CP-A to CP-C is modest (<5-fold) for substrates of OATPs that are predominately excreted unchanged in the bile,

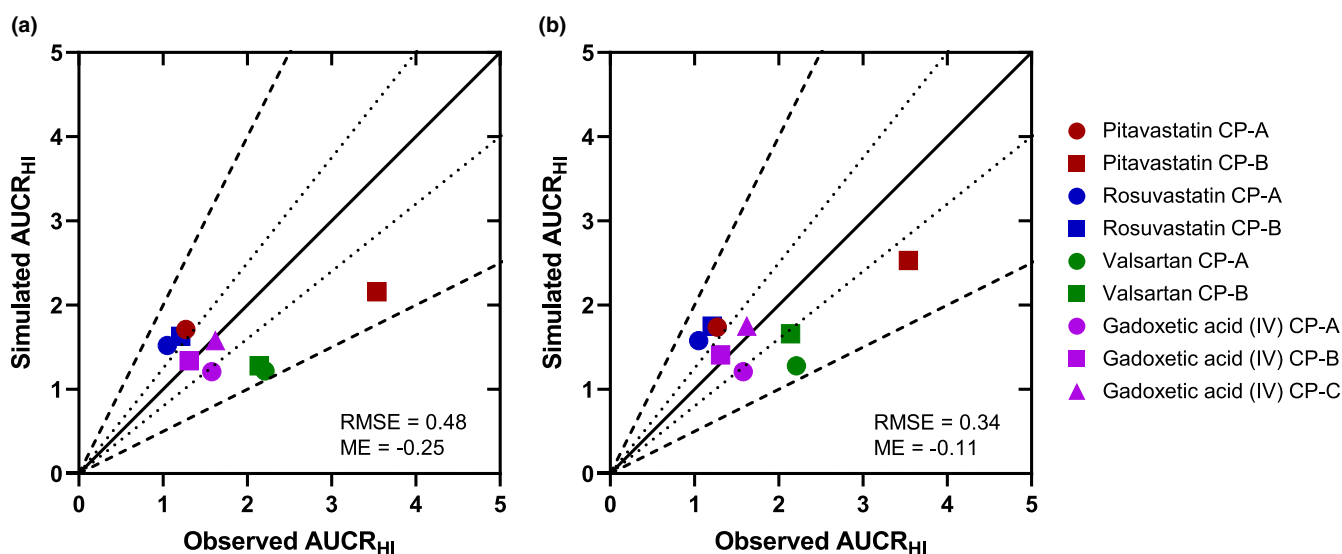


FIGURE 3 PBPK modeling achieves relatively good predictions of the $AUCR_{HI}$ for poorly metabolized OATP substrates (pitavastatin, rosuvastatin, valsartan, and gadoxetic acid). Simulations using PBPK modeling were done in Simcyp version 21, without (a) and with (b) incorporation of changes in transporter abundance at the cellular level. In both cases, the PBPK models included loss of functional liver volume (Table 3). Apart from gadoxetic acid administered i.v., all drugs were administered orally. The continuous lines represent the lines of unity, the dotted lines represent the bioequivalence prediction range (i.e., $AUCR_{HI}$ P/O ranging 0.8–1.25) and the dashed lines represent the two-fold prediction range (i.e., $AUCR_{HI}$ P/O ranging 0.5–2). $AUCR_{HI}$, ratio of area under the plasma concentration–time profile (AUC) in hepatic impairment subjects versus healthy volunteers; CP-A, Child-Pugh A; CP-B, Child-Pugh B; CP-C, Child-Pugh C; ME, mean error; PBPK, physiologically-based pharmacokinetic; RMSE, root mean square error.

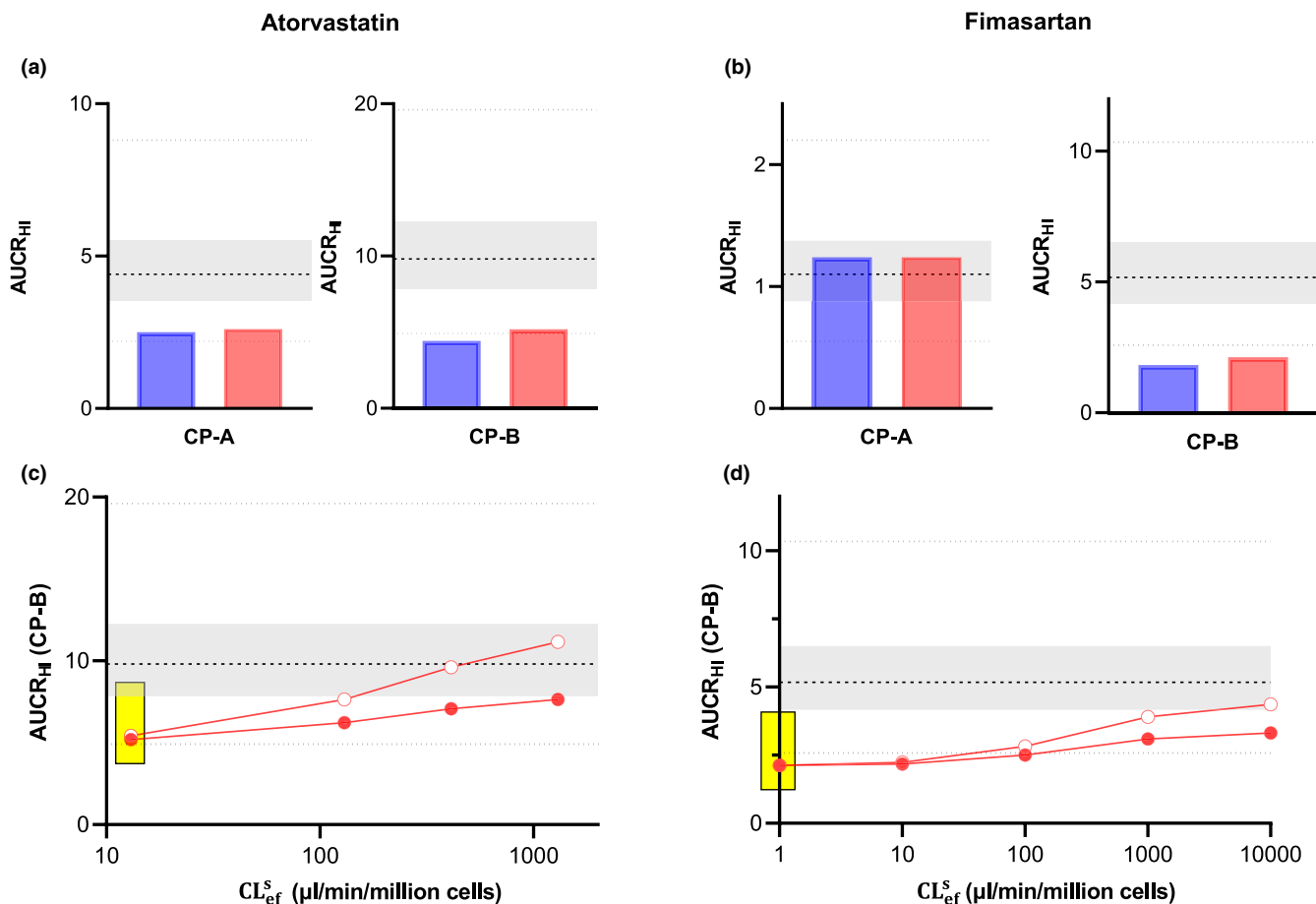


FIGURE 4 Prediction of atorvastatin (a, c) and fimasartan (b, d) $AUCR_{HI}$ using PBPK modeling improved by increasing the extent of sinusoidal efflux (CL_{ef}^s) and by affecting the directionality of the change in CL_{ef}^s in HI. (a, b) Simulations were conducted with Simcyp version 21 using one of two scenarios in HI: using the default reduction in functional liver volume without (blue bars) and with incorporation of changes in hepatic transporter abundance at the cellular level (red bars; Table 2). (c, d) Predictions of $AUCR_{HI}$ in CP-B were improved by increasing the CL_{ef}^s of the drug (i.e., before incorporating the effect of HI). Empty and full symbols respectively show simulations where sinusoidal efflux was assumed to be mediated predominately (90%) by MRP3 (and MRP3 abundance was increased in HI²) or only by passive diffusion (decreased in HI due to loss of functional liver volume; see text for details). Initial CL_{ef}^s values and resulting simulated $AUCR_{HI}$ are highlighted in the yellow box. The dashed lines represent the observed mean value (refs. 26,27) and dotted lines and shaded gray area represent the twofold and 1.25-fold (i.e., bioequivalence) prediction ranges, respectively. $AUCR_{HI}$, ratio of area under the plasma concentration–time profile (AUC) in hepatic impairment subjects versus healthy volunteers; CP, Child-Pugh.

it can be large (>10) for drugs that are metabolized by CYP3A4 enzymes (Table 1). Our simulations of $AUCR_{HI,u}$ using the extended clearance model, for virtual OATP/CYP3A4 model drug compounds administered i.v. and p.o. provide an explanation for this differential effect of hepatic impairment on OATP substrates:

- For most (if not all) OATP substrate drugs, it is likely that $RDS_{CL,H} = \text{all}$ rather than $RDS_{CL,H} = \text{uptake}$; therefore the magnitude of $AUCR_{HI,u}$ is sensitive to the ratio $CL_{ef}^s / (CL_{met} + CL_{ef}^c)$. $RDS_{CL,H} = \text{uptake}$ is often assumed for low permeability compounds (i.e., $CL_{ef}^s \ll CL_{met} + CL_{ef}^c$; in which case, sinusoidal

efflux is assumed to be mediated by passive diffusion). However, we recently showed, using positron emission tomography imaging, that this is not true for the classical low permeability OATP-substrate, rosuvastatin.²⁹ When $RDS_{CL,H} = \text{all}$, $AUCR_{HI,u}$ is larger than when $RDS_{CL,H} = \text{uptake}$, because the modulation of all hepatobiliary CLs in HI is responsible for the reduced hepatic CL of drugs in HI (Figure 1). In this case, the greater the ratio $CL_{ef}^s / (CL_{met} + CL_{ef}^c)$, the greater the $AUCR_{HI,u}$, until a plateau is reached for very large CL_{ef}^s (Figure 2a,b).

- When $RDS_{CL,H} = \text{all}$ and hepatic elimination is driven primarily by CYP3A4 metabolism, $AUCR_{HI,u}$ can be

large because of the larger decrease in hepatic CYP3A4 abundance in HI (Figure S9). This likely explains the larger $AUCR_{HI}$ values (>10) reported for dual OATP/CYP3A4 vs. OATP/BET substrates (Table 1). This effect is amplified with oral administration when the drug is also highly extracted by intestinal CYP3A4 metabolism. In that event, F_G (in HVs) will be low and therefore $AUCR_{HI,u}$ will likely be sensitive to any decrease in gut CYP3A4 abundance caused by HI (Figure 2c,d). Note that we focused here on CYP3A metabolism, but this may apply to substrates of other enzymes that are relevant for both liver and gut metabolism (such as uridine 5'-diphospho-glucuronosyltransferases; see Table 1).

- When $RDS_{CL,H} = \text{all}$ and hepatic elimination is mainly driven by biliary excretion of the unchanged drug, $AUCR_{HI,u}$ is limited by the lower impact of HI on the abundance of biliary efflux transporters (vs. impact on hepatic enzymes, such as CYP3A4; Figure S9). This likely explains the smaller $AUCR_{HI}$ values (<5) reported for OATP substrates (Table 1).
- When $RDS_{CL,H} = \text{all}$, the directionality (i.e., increase/decrease) of the modulation of CL_{ef}^s in HI significantly affects the $AUCR_{HI,u}$. Indeed, an increase in CL_{ef}^s in HI (as a result of increased abundance of sinusoidal efflux transporters²) further magnifies the effect of reducing hepatic elimination on drug CL (i.e., increases $AUCR_{HI,u}$; Figure 2b–d). Oppositely, a decrease in CL_{ef}^s in HI (e.g., if it is mediated only by passive diffusion; Figure 2a–c) increases drug CL and its dependency on CL_{in}^s and therefore reduces $AUCR_{HI,u}$. This is of particular interest as there are conflicting data from different groups regarding the directionality of the modulation of the abundance of sinusoidal efflux transporters (MRP3 and MRP4) in HI: in-house data from our group suggest that MRP3 abundance increases in HI, whereas others using a different peptide for quantification have shown a downregulation of the transporter in HI^{2,3,30}; similarly MRP4 abundance was shown to be increased by some³ whereas reduced by others.³⁰

These insights from the extended clearance model were leveraged to improve PBPK M&S predictions of $AUCR_{HI}$ for the two dual OATP/CYP3A4 substrates, atorvastatin and fimasartan. Indeed, whereas the $AUCR_{HI}$ of OATP/BET substrates pitavastatin, rosuvastatin, valsartan, and gadoxetic acid was relatively well-predicted by PBPK M&S (Simcyp version 21; Figure 3), there was a trend towards underprediction for the two dual OATP/CYP3A4 substrates (Figure 4a,b). An important challenge of PBPK model development for hepatic transporter substrates is the inability to definitively estimate all hepatobiliary CLs, including CL_{ef}^s

(unless imaging data are available). Therefore, for atorvastatin, we assumed that its hepatic sinusoidal efflux was mediated only by passive diffusion (see atorvastatin model development in Appendix S1). For fimasartan, because only limited data were available, we estimated $CL_{int,uptake}$ from the intravenous drug CL, assuming that $RDS_{CL,H} = \text{uptake}$ (see fimasartan model development in Appendix S1). Therefore, CL_{ef}^s was assumed to be negligible. Because these assumptions might not hold true (in particular, for atorvastatin, there is a report of active transport by MRP3³¹), we investigated the impact of changing the CL_{ef}^s values on the $AUCR_{HI}$ for these two drugs. Increasing CL_{ef}^s of atorvastatin and fimasartan moved the $AUCR_{HI}$ into or closer to the bioequivalence range (Figure 4c,d). In addition, the predictions were further improved when CL_{ef}^s was assumed to be mediated primarily (90%) by MRP3 (and its abundance was increased in HI²). Whether MRP3 or MRP4 contributes to the sinusoidal efflux of the two drugs, and, if so, the fraction-transported (f_i) of this contribution, is unclear and needs further investigation.

There are a few limitations to this work. First, PBPK model development and verification can be challenging for transporter substrates as it is often difficult to determine and verify the absolute values of the hepatobiliary CLs estimates, and the relative contribution of different transporters (influx and efflux) and drug metabolizing enzymes. Only for rosuvastatin and gadoxetic acid were clinical imaging data available that were used to back-calculate the in vitro hepatic influx and efflux CLs estimates (Appendix S1). Although PBPK model fits in HV were deemed satisfying for our application, we acknowledge that PBPK models could be further improved (e.g., pitavastatin). This will likely involve a better characterization of the hepatobiliary CLs of drugs. Whereas the bottom-up in vitro in vivo extrapolation approaches were used to estimate the relative contribution of transporters to hepatic uptake and efflux (e.g., rosuvastatin or pitavastatin), data were not always available to do so (e.g., gadoxetic acid and fimasartan). Therefore, caution should be used when interpreting data from the PBPK models regarding the assumptions made (e.g., assuming $RDS_{CL,H} = \text{uptake}$, or that a CL pathways is mediated 100% by a given transporter; see Appendix S1). The simulations presented are only for illustration of given principles and the models presented need further validation (including perturbation of metabolism/transport pathways by validated in vivo inhibitors/inducers). Second, besides the blood AUC of drugs, it is important to consider the impact of HI on drug concentrations at the site of efficacy and toxicity. For example, irrespective of the RDS, the hepatic AUC is dependent on the metabolic and canalicular efflux CLs, but not on CL_{in}^s or CL_{ef}^s ,

unless there is significant extrahepatic elimination, as previously noted.¹⁷ Third, this work used the extended clearance model (derived from the well-stirred model) to simulate the effect of HI on the AUC of transported drugs, and the authors acknowledge the limitations of using the well-stirred model for high extraction compounds. Extreme scenarios where CL_{met} and/or CL_{ef}^s are very large might be better described by other models. However, it is unlikely that the overall conclusions of this paper would be affected by the use of a different model. Fourth, in this study, we assumed that changes in transporter-mediated and metabolic clearances were driven by changes in DMET abundance. Such changes can also be the result of changes in the DMET affinity for drugs.

In conclusion, simulations of $AUCR_{HI,u}$ for different scenarios using the extended clearance model have provided a better understanding of factors that drive $AUCR_{HI,u}$ for dual OATP/CYP3A4 substrates, for which large $AUCR_{HI}$ have been reported. In addition, principles derived from this work can be applied to substrates of other DMETs when abundance data (e.g., obtained by proteomics³²) are available to inform predictions. This work emphasizes the need to obtain accurate estimates of all hepatobiliary CLs of drugs, including CL_{ef}^s , to accurately predict the effect of HI (and the effect of other intrinsic and extrinsic factors) on drug blood AUC. Assuming $RDS_{CL,H} = \text{uptake}$ based on permeability data alone is likely not justified (see considerations on rosuvastatin above). In this regard, imaging data (when available) and in vitro–in vivo extrapolation methods (in particular, proteomics-informed)³³ can be used to obtain such estimates.

AUTHOR CONTRIBUTIONS

All authors wrote the manuscript. F.S., M.K.L., and J.D.U. designed the research. F.S. performed the research. F.S., M.K.L., and J.D.U. analyzed the data.

ACKNOWLEDGMENTS

The authors thank members of the Unadkat laboratory for valuable discussion, as well as Dr. Loeckie de Zwart (Janssen Pharmaceuticals) for her insightful suggestions on the manuscript.

FUNDING INFORMATION

This research was supported by the University of Washington Research Affiliate Program on Transporters (UWRAPT), funded by Gilead Sciences, Amgen, Takeda, and Janssen Pharmaceuticals.

CONFLICT OF INTEREST STATEMENT

X.L., Y.L., P.C., O.E., and R.E. are/were employees of their respective companies and received stocks or stock options

from their companies. All other authors declared no competing interests for this work.

ORCID

Yurong Lai  <https://orcid.org/0000-0001-9505-333X>

Jashvant D. Unadkat  <https://orcid.org/0000-0002-4820-8455>

REFERENCES

1. Prasad B, Bhatt DK, Johnson K, et al. Abundance of phase 1 and 2 drug-metabolizing enzymes in alcoholic and hepatitis C cirrhotic livers: a quantitative targeted proteomics study. *Drug Metab Dispos.* 2018;46:943-952.
2. Wang L, Collins C, Kelly EJ, et al. Transporter expression in liver tissue from subjects with alcoholic or hepatitis C cirrhosis quantified by targeted quantitative proteomics. *Drug Metab Dispos.* 2016;44:1752-1758.
3. El-Khateeb E, Achour B, Al-Majdoub ZM, Barber J, Rostami-Hodjegan A. Non-uniformity of changes in drug-metabolizing enzymes and transporters in liver cirrhosis: implications for drug dosage adjustment. *Mol Pharm.* 2021;18:3563-3577.
4. Johnson TN, Boussery K, Rowland-Yeo K, Tucker GT, Rostami-Hodjegan A. A semi-mechanistic model to predict the effects of liver cirrhosis on drug clearance. *Clin Pharmacokinet.* 2010;49:189-206.
5. Verbeeck RK. Pharmacokinetics and dosage adjustment in patients with hepatic dysfunction. *Eur J Clin Pharmacol.* 2008;64:1147-1161.
6. U.S. Food and Drug Administration. Guidance for industry: pharmacokinetics in patients with impaired hepatic function: study design, Data Analysis, and Impact on Dosing and Labeling. 2003.
7. European Medicines Agency. Guideline on the evaluation of the pharmacokinetics of medicinal products in patients with impaired hepatic function. 2005.
8. Lin W, Chen Y, Unadkat JD, Zhang X, Wu D, Heimbach T. Applications, challenges, and outlook for PBPK modeling and simulation: a regulatory, industrial and academic perspective. *Pharm Res.* 2022;39:1701-1731.
9. Chu X, Prasad B, Neuhoof S, et al. Clinical implications of altered drug transporter abundance/function and PBPK modeling in specific populations: an ITC perspective. *Clin Pharmacol Ther.* 2022;112:501-526. doi:10.1002/cpt.2643
10. Heimbach T, Chen Y, Chen J, et al. Physiologically-based pharmacokinetic modeling in renal and hepatic impairment populations: a pharmaceutical industry perspective. *Clin Pharmacol Ther.* 2021;110:297-310.
11. Ladumor MK, Storelli F, Liang X, et al. Predicting changes in the pharmacokinetics of CYP3A-metabolized drugs in hepatic impairment and insights into factors driving these changes. *CPT Pharmacometrics Syst Pharmacol.* 2022;12:261-273. doi:10.1002/psp4.12901
12. Lin J, Kimoto E, Yamazaki S, et al. Effect of hepatic impairment on OATP1B activity: quantitative pharmacokinetic analysis of endogenous biomarker and substrate drugs. *Clin Pharmacol Ther.* 2023;113:1058-1069. doi:10.1002/cpt.2829
13. McFeely SJ, Ritchie TK, Yu J, Nordmark A, Levy RH, Ragueneau-Majlessi I. Identification and evaluation of clinical substrates of organic anion transporting polypeptides 1B1 and 1B3. *Clin Transl Sci.* 2019;12:379-387.

14. Hachad H, Ragueneau-Majlessi I, Levy RH. A useful tool for drug interaction evaluation: the University of Washington Metabolism and Transport drug interaction database. *Hum Genomics*. 2010;5:61-72.
15. Whirl-Carrillo M, Huddart R, Gong L, et al. An evidence-based framework for evaluating pharmacogenomics knowledge for personalized medicine. *Clin Pharmacol Ther*. 2021;110:563-572.
16. Sirianni GL, Pang KS. Organ clearance concepts: new perspectives on old principles. *J Pharmacokinet Biopharm*. 1997;25:449-470.
17. Patilea-Vrana G, Unadkat JD, Transport v. Metabolism: what determines the pharmacokinetics and pharmacodynamics of drugs? Insights from the extended clearance model. *Clin Pharmacol Ther*. 2016;100:413-418.
18. Shitara Y, Horie T, Sugiyama Y. Transporters as a determinant of drug clearance and tissue distribution. *Eur J Pharm Sci*. 2006;27:425-446.
19. Benet LZ, Bowman CM, Liu S, Sodhi JK. The extended clearance concept following Oral and intravenous dosing: theory and critical analyses. *Pharm Res*. 2018;35:242.
20. Yang J, Jamei M, Yeo KR, Tucker GT, Rostami-Hodjegan A. Prediction of intestinal first-pass drug metabolism. *Curr Drug Metab*. 2007;8:676-684.
21. Jamei M, Marciniak S, Feng K, Barnett A, Tucker G, Rostami-Hodjegan A. The Simcyp® population-based ADME simulator. *Expert Opin Drug Metab Toxicol*. 2009;5:211-223.
22. Hui CK, Cheung BMY, Lau GKK. Pharmacokinetics of pitavastatin in subjects with child-Pugh a and B cirrhosis. *Br J Clin Pharmacol*. 2005;59:291-297.
23. Simonson SG, Martin PD, Mitchell P, Schneck DW, Lasseter KC, Warwick MJ. Pharmacokinetics and pharmacodynamics of rosuvastatin in subjects with hepatic impairment. *Eur J Clin Pharmacol*. 2003;58:669-675.
24. Brookman LJ, Rolan PE, Benjamin IS, et al. Pharmacokinetics of valsartan in patients with liver disease. *Clin Pharmacol Ther*. 1997;62:272-278.
25. Gschwend S, Ebert W, Schultze-Mosgau M, Breuer J. Pharmacokinetics and imaging properties of Gd-EOB-DTPA in patients with hepatic and renal impairment. *Invest Radiol*. 2011;46:556-566.
26. Kim CO, Lee HW, Oh ES, et al. Influence of hepatic dysfunction on the pharmacokinetics and safety of fimasartan. *J Cardiovasc Pharmacol*. 2013;62:524-529.
27. Gibson D et al. Effects of hepatic and renal impairment on pharmacokinetics (PK) and pharmacodynamics (PD) of atorvastatin. *Pharm Res*. 1996;13(Suppl 9):S428.
28. Blaschke TF. Protein binding and kinetics of drugs in liver diseases. *Clin Pharmacokinet*. 1977;2:32-44.
29. Billington S, Shoner S, Lee S, et al. Positron emission tomography imaging of [¹¹C]rosuvastatin hepatic concentrations and hepatobiliary Transport in humans in the absence and presence of cyclosporin a. *Clin Pharmacol Ther*. 2019;106:1056-1066.
30. Drozdzik M, Szelag-Pieniek S, Post M, et al. Protein abundance of hepatic drug transporters in patients with different forms of liver damage. *Clin Pharmacol Ther*. 2020;107:1138-1148.
31. Deng F, Tuomi SK, Neuvonen M, et al. Comparative hepatic and intestinal efflux transport of statins. *Drug Metab Dispos*. 2021;49:750-759.
32. Prasad B, Achour B, Artursson P, et al. Toward a consensus on applying quantitative liquid chromatography-tandem mass spectrometry proteomics in translational pharmacology research: a white paper. *Clin Pharmacol Ther*. 2019;106:525-543.
33. Storelli F, Yin M, Kumar AR, et al. The next frontier in ADME science: predicting transporter-based drug disposition, tissue concentrations and drug-drug interactions in humans. *Pharmacol Ther*. 2022;238:108271.
34. Varma MV, Bi Y, Kimoto E, Lin J. Quantitative prediction of transporter- and enzyme-mediated clinical drug-drug interactions of organic anion-transporting polypeptide 1B1 substrates using a mechanistic net-effect model. *J Pharmacol Exp Ther*. 2014;351:214-223.
35. Patilea-Vrana GI, Unadkat JD. When does the rate-determining step in the hepatic clearance of a drug switch from sinusoidal uptake to all hepatobiliary clearances? Implications for predicting drug-drug interactions. *Drug Metab Dispos*. 2018;46:1487-1496.

SUPPORTING INFORMATION

Additional supporting information can be found online in the Supporting Information section at the end of this article.

How to cite this article: Storelli F, Ladumor MK, Liang X, et al. Toward improved predictions of pharmacokinetics of transported drugs in hepatic impairment: Insights from the extended clearance model. *CPT Pharmacometrics Syst Pharmacol*. 2024;13:118-131. doi:[10.1002/psp4.13062](https://doi.org/10.1002/psp4.13062)